



## A zirconium oxide film self-assembled at the air–water interface

M.J. Henderson<sup>a</sup>, A. Gibaud<sup>b</sup>, J.-F. Bardeau<sup>b</sup>, A.R. Rennie<sup>c</sup>, J.W. White<sup>a,\*</sup>

<sup>a</sup>Research School of Chemistry, Australian National University, Canberra, ACT 0200, Australia

<sup>b</sup>Laboratoire de Physique de l'Etat Condensé, UMR CNRS 6087, Université du Maine, 72085, Le Mans, Cedex 09, France

<sup>c</sup>Uppsala University, The Studsvik Neutron Research Laboratory, S-611 82 Nyköping, Sweden

### Abstract

A self-assembled zirconia-based film, produced at the air–water interface using sodium dodecyl sulphate (SDS) as the template, has been characterised by energy-dispersive X-ray reflectometry, X-ray diffraction, and X-ray fluorescence analysis. Long-range order due to the lamellar liquid crystalline arrangement of the surfactant micelles was significant enough to produce Bragg diffraction. X-ray fluorescence from the specimens in the electron microscope indicates that the principal component of the film contains zirconium, oxygen and sulphate, -suggesting that the film contains zirconium polyoxo ions and surfactant. Raman spectroscopy indicates the presence of a zirconium hydroxide.

© 2004 Elsevier B.V. All rights reserved.

PACS: 61.10.Kw; 68.03.Hj; 81.16.Dn

Keywords: Zirconium oxide; Thin film; Air–water interface; Time-resolved X-ray reflectometry

### 1. Introduction

Zirconia is an important functional material. It is used in catalysis, e.g., for the isomerization of alkenes [1], or in optics for smart thermo- [2] or electro- [3] optical modulation. The ability to produce porous zirconium oxide with a high surface area via a template route either as a powder [4–6] or as structurally uniform thin films [7–11] is therefore of interest.

Our focus is the production of highly orientated films at the air–water interface. This interface has been used previously to prepare two-dimensional arrays of inorganic compounds including calcium carbonate, [12] titania [13,14] and zirconia [11,13,15]. The utility of a surfactant assembly as template for the production of inorganic materials at the air–water interface is illustrated by hexadecyltrimethylammonium halide, C<sub>16</sub>TAX (X = Cl, Br), -templated silica [16–18] and more recently sodium dodecyl sulphate SDS-templated titania [19,20]. The titania-based film, prepared from an acidic solution of a titanium alkoxide, Ti(OBu<sup>n</sup>)<sub>4</sub>,

\*Corresponding author. Fax.: +61 2 6125 4903.

E-mail address: [jww@rsc.anu.edu.au](mailto:jww@rsc.anu.edu.au) (J.W. White).

and SDS, shows Bragg diffraction consistent with a lamellar mesostructure in which the film components, titania and dodecyl sulphate exhibit a regular 35 Å arrangement. In this paper, we present our work on the preparation and characterisation of the analogous zirconia-based film.

Mesoporous zirconias have been prepared as powders from zirconium alkoxides and aliphatic anionic surfactants containing a sulphate head-group, including sodium hexadecyl sulphonate [21] and SDS [21,22]. When bitailed sodium-7-ethyl-2-methyl-undecyl-sulphonate was used as the template [23,24], a microporous solid was obtained. To our knowledge, our work here offers the first report of an ordered zirconia film self-assembled at the air–water interface using a surfactant assembly as the template.

## 2. Experimental procedure

### 2.1. Chemicals

Milli-Q<sup>®</sup> water was used for all film syntheses. Zirconium (IV) *n*-butoxide (Aldrich, 80% solution in butanol), hydrochloric acid (36–39% w/w) and alizarin (BDH) were used as received. SDS (Lancaster 99%) was recrystallised from hot water:ethanol (1:9).

### 2.2. Synthesis

A film was produced using the following millimolar ratios of H<sub>2</sub>O:HCl:Zr(OBu<sup>*n*</sup>)<sub>4</sub>:SDS, 100:0.6–1.2:0.15:0.05–0.08, at times between 1 h at 80 °C or 2 weeks at room temperature. Where a room temperature synthesis was performed, e.g., for the film used for GISAX analysis, film formation was facilitated by the addition of water about 1 week into the experiment.

A typical preparation is as follows. Zirconium (IV) butoxide (0.28 g) was added to hydrochloric acid (36–39% w/w, 0.48 g) and the mixture stirred for 10 min. The thick white precipitate was treated with water (0.45 g) until the precipitate dissolved to give a clear and colourless solution. This solution was then transferred to a Nalgene bottle. A solution of SDS (0.09 g) in water (6.9 g) was

poured gently over the zirconium-containing solution causing some precipitation. The container was sealed and left undisturbed until the mixture began to clarify 2 h at room temperature. The solution was then heated to 80 °C for 1 h. After allowing any precipitate to settle, the material at the interface was retrieved by gently adding water to raise the film high enough to be transferred to a glass substrate. A film examined *ex situ* was the insoluble part of the film remaining after it had been bathed in water and then allowed to dry in air. The rinsed film is assumed to contain only surfactant that is anchored firmly to the inorganic component of the film.

### 2.3. Energy-dispersive reflectometry

The energy-dispersive experiment was performed at 25 °C in the Research School of Chemistry at the Australian National University, using the instrument described elsewhere [19,20] in a sealed temperature-controlled Teflon trough (140 × 40 × 2 mm). The data were recorded as X-ray reflectivity, *I*, as a function of scalar momentum transfer,

$$q_z = \frac{4\pi}{\lambda} \sin \theta, \quad (1)$$

where  $\lambda$  is the X-ray wavelength and  $\theta$  the specular reflectance angle (0.6°). The incident angle was evaluated experimentally by recording the specular Bragg reflections from a highly ordered mesostructured silicate film templated at the air–water interface by hexadecyltrimethylammonium chloride, C<sub>16</sub>TAC [17]. The trough was hermetically sealed to maintain a constant vapour pressure above the interface. Maestro software (Maestro<sup>®</sup>-32, EG & G<sup>®</sup>) was used to record the energy-dispersive reflectivity profiles at 5 min intervals.

### 2.4. Scanning electron microscopy (SEM) and X-ray fluorescence spectroscopy

Measurements were performed using a Jeol 6400 microscope. The sample was gold-coated prior to analysis to prevent charging. The result of the

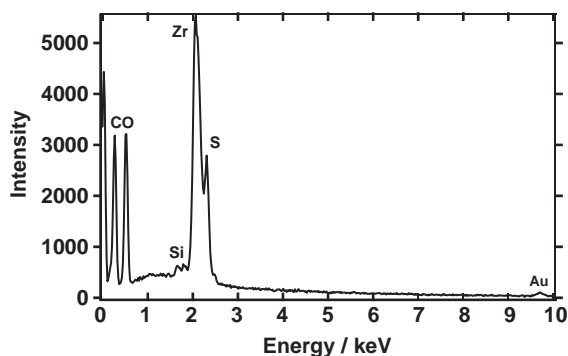


Fig. 1. X-ray fluorescence analysis of a zirconia-based film obtained at the air–water interface from an acidic solution of  $Zr(OBu^t)_4$  and SDS.

X-ray fluorescence spectroscopic analysis is presented in Fig. 1.

### 2.5. X-ray diffraction (XRD)

Diffraction patterns were measured with a Philips X'Pert Materials Research Diffractometer equipped with a humidity-controlled cell, using monochromatic  $Cu_{K\alpha}$  radiation operated at 40 kV and 30 mA.

### 2.6. Grazing incidence small-angle X-ray scattering (GISAXS)

The pattern was obtained on the X22B beamline at the National Synchrotron Light Source, Brookhaven National Laboratory, US.

### 2.7. Raman spectroscopy

Raman spectra were measured using a Horiba T64000 instrument calibrated using the spectrum obtained from diamond ( $1332\text{ cm}^{-1}$ ).

## 3. Results and discussion

To perform the time-resolved experiment at the air–water interface, an aqueous acidic zirconia solution was placed in evenly spaced aliquots across the area of the trough. Fast mixing was achieved by pouring the aqueous surfactant

solution on top of these drops to bring the level just over the lip of the trough. The trough lid was then secured and the energy-dispersive reflectivity profile was recorded at 5 min intervals over an 86 h period. The data were recorded as reflectivity intensity  $I$ , as a function of scalar momentum transfer  $q_z$ .

The first spectrum recorded displayed a broad Bragg peak between  $q_z = 0.18$  and  $0.19\text{ \AA}^{-1}$ . The intensity of the peak gradually lessened until, after about 2 h, only a fringe characteristic of surfactant was noticeable. A sharp Bragg peak at  $q_z = 0.19\text{ \AA}^{-1}$  appeared 2.75 h into the experiment and continued to develop until at 36 h a fall in the count rate was noted. The period following the drop in the count rate was characterised by a shift in the Bragg peak position from  $q_z = 0.19$  to  $q_z = 0.18\text{ \AA}^{-1}$ , corresponding to a change in the  $d$  spacing from 33 to 35  $\text{\AA}$ . The  $I$  vs.  $q_z$  vs.  $t$  profiles for this period where the Bragg peak shifted are shown in Fig. 2. Beyond this time, the Bragg peak at  $q_z = 0.18\text{ \AA}^{-1}$  was established and the intensity increased dramatically until the experiment was terminated. We attribute this behaviour to the incorporation of a cosurfactant, dodecanol, produced from the hydrolysis of SDS [25] into the film as reported for a titania-based film self-assembling at the air–water interface [19].

A chemical spot test for zirconium [26] using an alcoholic solution of alizarin dye on a film that was

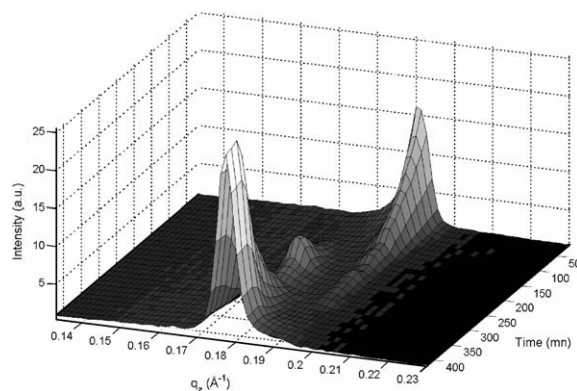


Fig. 2. Energy-dispersive X-ray  $I$  versus  $q_z$  versus  $t$  profiles of a zirconia-based film self-assembling at the air–water interface showing a change in the Bragg peak position. Angle of incidence,  $\theta = 0.6^\circ$ .

removed from the interface and then rinsed and dried was positive, suggesting that zirconia within the film was accessible for chemical post-treatment. Post-functionalisation of mesoporous zirconia-based films using organic ligands has been reported previously [10]. SEM images of the synthesised zirconia film (not shown) show that the film surface was smooth. An X-ray fluorescence analysis of the zirconia-based film, Fig. 1, indicated that carbon, oxygen, sulphur and zirconium were present.

The XRD pattern, Fig. 3(a), shows a pattern consistent with a structure having a lamellar alternation of surfactant and oxide layers. The reflections could not be indexed to other unit cells, e.g., that for hexagonal mesostructuring as demonstrated for surfactant templated zirconia, [6] alumina [27] and titania [28] as the (100), (110) and (200) diffraction peaks of this unit cell were absent. Similarly, a cubic unit cell was ruled out [28]. The lamellar ordering of the zirconia film was confirmed by a GISAX measurement, Fig. 4. The  $d$  spacing, 36 Å, is in agreement with that reported for a titania-based film produced at the air–water interface [19,20] and that of a silica-based film obtained by a dip-coating process from a sol containing tetraethoxysilane and SDS [29]. We note here that a small-angle X-ray scattering pattern (not shown) displayed (001) and (002) diffraction peaks of the lamellar phase. An estimate of the extent of the regular layer lattice was obtained from the broadening of the first diffraction peak using the treatment of Warren [30]. If  $\theta$  is the Bragg angle and  $\beta$  the full width of the peak at half maximum intensity in radians, the coherence length  $L_c$  is

$$L_c = \frac{0.89\lambda}{\beta \cos \theta}, \quad (2)$$

where  $\lambda$  is the incident wavelength. The coherence length obtained was 2017 Å, more than twice the length obtained for a mesostructured silica-SDS film [29]. The coherence length is significantly smaller than the thickness of the film as revealed by SEM cross-section. This result suggests that the value is a lower limit of the degree of long-range ordering of the ZrO<sub>2</sub>-SDS layers.

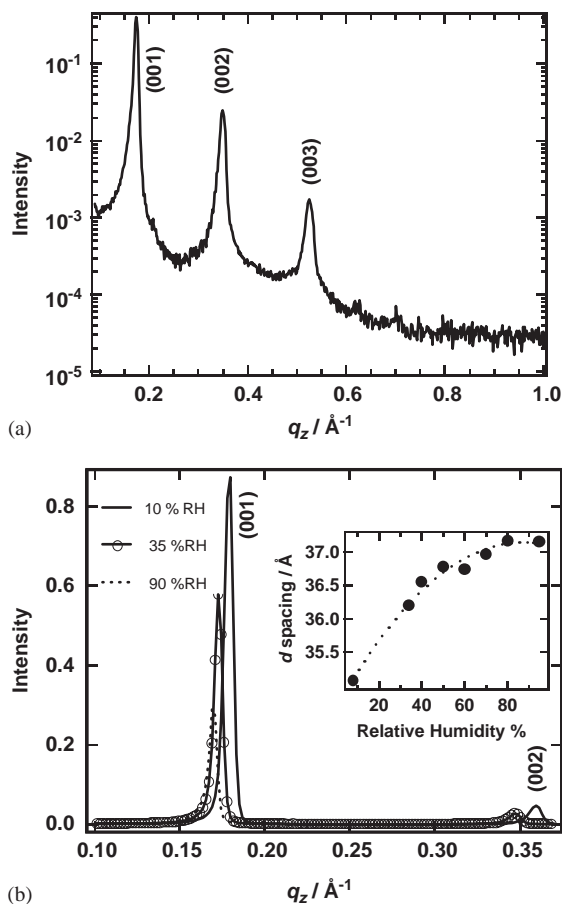


Fig. 3. (a) X-ray diffraction pattern of a zirconia-based film obtained at the air–water interface. (b) X-ray diffraction patterns of a zirconia-based film at relative humidity 10% (solid line), 35% (solid line, circle) and 90% (dot line). Inset shows a plot of the response of film  $d$  spacing to relative humidity. The line is a guide to the eye.

The change in the first two orders of diffraction as a result of swelling the film at increasing humidity is shown in Fig. 3(b). The data correspond to relative humidities 10% (solid line), 35% (solid line, circle) and 90% (dot line). The inset of Fig. 3(b) shows the change in  $d$  spacing evaluated from the (001) diffraction peak plotted as a function of relative humidity. The film was first measured in 50% relative humidity. The film was then saturated in 95% relative humidity before reducing the humidity to about 10%. Thereafter, the humidity was raised to 35, 50, 60, 70 and

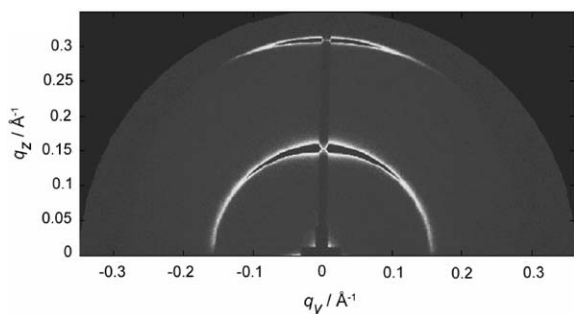


Fig. 4. GISAX pattern of a zirconia-based film obtained at the air–water interface from an acidic solution of  $\text{Zr}(\text{OBU}^n)_4$  and SDS.

finally 80%. This large swelling is an interesting pointer to the structure of the zirconium oxide layer since hydration of the SDS headgroups alone might be expected to produce a contraction of the layer spacing (due to a change in the chain tilt angle) as it does in SDS crystalline phases [31]. The change in the tilt angle from  $15^\circ$  (with respect to the long axis of the anion and the unit cell) in anhydrous SDS to  $45^\circ$  for the monohydrate represents a  $5 \text{ \AA}$  change in the lamellar thickness. However, the effect of increasing the hydration state of the crystalline phases of SDS is to decrease the lamellar thickness, an effect attributed to electrostatic interactions between the headgroups that in turn affect the alignment of the tails. In contrast, the lamellar thickness of the mesostructured zirconia-based film presented in this study increases with increasing humidity. We conclude that although a change in tilt angle might have occurred during hydration, the layer lattice change is dominated by the swelling.

Although the effect of temperature of the film mesostructure was outside the scope of this study, heat is also known to induce phase transformations of mesostructured metal oxides [32]. This behaviour is illustrated by the hexagonal to lamellar transformation of aluminophosphate, templated in alcoholic solution by dodecyl phosphate, between the rather low temperature range of  $35\text{--}43^\circ\text{C}$  [33]. We note that the preparation of the aluminophosphate in aqueous media between  $20$  and  $120^\circ\text{C}$  yielded exclusively the lamellar

phase. All of the characterisation experiments of the zirconia-based film here, including XRD and GISAXS, were performed at ambient temperature below  $30^\circ\text{C}$ . As these experiments indicated a lamellar ordering of zirconium oxide and dodecyl sulphate, there was no evidence to suggest that a phase transformation caused by heat has contributed measurably to the diffraction signals.

Increased humidity decreased the intensity greatly for both orders without significant change in their width. This is consistent with a reduction in contrast between the zirconium oxide and surfactant layer. An interesting possibility is the incorporation of the added water into the zirconium layer. Inspection of the estimated X-ray scattering length densities for  $\text{Zr}(\text{OH})_4$  ( $3.88 \times 10^{-5} \text{ \AA}^{-2}$ ), SDS ( $0.93 \times 10^{-5} \text{ \AA}^{-2}$ ) and water ( $0.94 \times 10^{-5} \text{ \AA}^{-2}$ ) supports this hypothesis. For the estimation, the stoichiometry of the metal oxide was considered to be that of the uncondensed hydroxide  $\text{Zr}(\text{OH})_4$  with a density of  $4.8 \text{ g cm}^{-3}$ , a density reported for an amorphous hydrous zirconium oxide gel [34]. The contrast is only reduced significantly when water is added to the zirconia layer. The (001) intensity change to full hydration was a decrease by a factor of three so the contrast change was a factor of  $\sqrt{3}$ . Assuming that all the absorbed water enters the  $\text{Zr}(\text{OH})_4$  layer (considered an hydrophilic oligomer), this contrast change allows the mole percentage water in that layer to be evaluated as about 25%. The presence of a zirconium hydroxide within the film is supported by the Raman spectrum of the film material shown in Fig. 5. Though the Raman bands observed below  $600 \text{ cm}^{-1}$  are attributed to the vibration modes of Zr–O–Zr bonds, the lines do not correspond to those of either the cubic, monoclinic or tetragonal phases of zirconia [35]. However, the profile of the spectrum between  $100$  and  $600 \text{ cm}^{-1}$  does show some similarity with that obtained from a zirconium hydroxide gel precipitated from aqueous zirconyl chloride solution, pH 4 [36]. The absence of long-range order within the zirconium hydroxide can be reconciled with the order that gives rise to the diffraction peaks as the latter is not due to atomic ordering but to the lamellar liquid crystalline arrangement of the surfactant micelles.

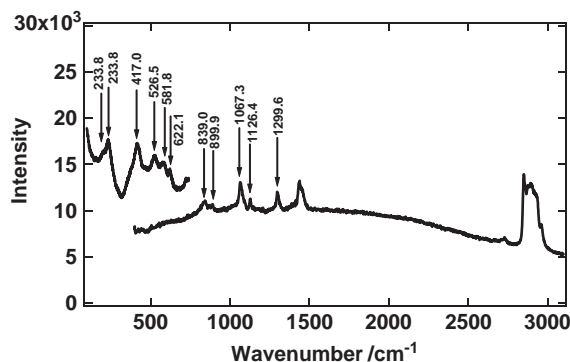


Fig. 5. Raman spectra of a zirconia-based film obtained at the air–water interface. Two wavelengths were used to obtain the full range, 514 nm (100–800  $\text{cm}^{-1}$ ) and 568 nm (400–3100  $\text{cm}^{-1}$ ).

In this paper, we have shown that an ordered zirconia-based film can be produced at the air–water interface by the template method. In a subsequent publication we present the results of a high-intensity neutron diffraction study of the zirconia-based film mounted onto a glass substrate in which a systematic variation in the contrast between the oxide and surfactant layers allowed the two or three diffraction orders shown by this system to be used for structural purposes.

### Acknowledgements

Financial support from an Innovation Access Programme (CG050120) administered by the Department of Education Science and Training is gratefully acknowledged. Messrs D. King and T. Dowling are thanked for their assistance with the energy-dispersive instrumentation. Dr. B. Ocko (National Synchrotron Light Source, Brookhaven National Laboratory) is acknowledged for experimental assistance at the X22B beamline.

### References

- [1] Y. Ono, *Catal. Today* 81 (2003) 3.
- [2] L.A. Chivacchi, C. Bourgaux, V. Briois, S.H. Pulcinelli, C.V. Santilli, *J. Appl. Cryst.* 33 (2000) 592.
- [3] A.K. Jonsson, G.A. Niklasson, M. Veszelei, *Thin Solid Films* 402 (2002) 242.
- [4] Z.Y. Yuan, A. Vantomme, A. Léonard, B.L. Su, *Chem. Commun.* (2003) 1558.
- [5] U. Ciesla, S. Schacht, G.D. Stucky, K.K. Unger, F. Schüth, *Angew. Chem. Int. Ed. Engl.* 35 (1996) 541.
- [6] P. Lui, J.S. Reddy, A. Adnot, A. Sayari, in: R.F. Lobo, J.S. Beck, S.L. Suib, D.R. Corbin, M.E. Davis, L.E. Iton, S.I. Zones (Eds.), *Microporous and Macroporous Materials*, vol. 431, Materials Research Society, Pittsburgh, 1996, pp. 101–110.
- [7] D.G. Shchukin, R.A. Caruso, *Adv. Funct. Mater.* 13 (2003) 789.
- [8] E.L. Crepaldi, G. Soler-Illia, D. Grosso, C. Sanchez, *New J. Chem.* 27 (2003) 9.
- [9] G.J.D. Soler-Illia, C. Sanchez, B. Lebeau, J. Patarin, *Chem. Rev.* 102 (2002) 4093.
- [10] E.L. Crepaldi, G. Soler-Illia, D. Grosso, P.A. Albouy, C. Sanchez, *Chem. Commun.* (2001) 1582.
- [11] I. Moriguchi, Y. Tsujigo, Y. Teraoka, S. Kagawa, *J. Phys. Chem. B* 104 (2000) 8101.
- [12] H.H. Wickman, J.N. Korley, *Nature* 393 (1998) 445.
- [13] I. Moriguchi, Y. Tsujigo, Y. Teraoka, S. Kagawa, *Adv. Mater.* 11 (1999) 997.
- [14] F. Facca, G. Puccetti, R.M. Leblanc, *Colloids Surf. A* 149 (1999) 89.
- [15] I. Moriguchi, Y. Tsujigo, Y. Teraoka, S. Kagawa, *J. Sol-Gel Sci. Technol.* (19) (2000) 227.
- [16] H. Yang, N. Coombs, I. Sokolov, G.A. Ozin, *Nature* 381 (1996) 589.
- [17] A.S. Brown, S.A. Holt, P.A. Reynolds, J. Penfold, J.W. White, *Langmuir* 14 (1998) 5532.
- [18] T. Brennan, A.V. Hughes, S.J. Roser, S. Mann, K.J. Edler, *Langmuir* 18 (2002) 9838.
- [19] M.J. Henderson, D. King, J.W. White, *Langmuir* 20 (2004) 2305.
- [20] M.J. Henderson, D. King, J.W. White, *Aust. J. Chem.* 56 (2003) 933.
- [21] E. Zhao, O. Hernández, G. Pacheco, S. Hardcastle, J.J. Fripiat, *J. Mater. Chem.* 8 (1998) 1635.
- [22] G. Pacheco, E. Zhao, A. Garcia, A. Sklyarov, J.J. Fripiat, *Chem. Commun.* (1997) 491.
- [23] G. Pacheco, J.J. Fripiat, *J. Phys. Chem. B* 104 (2000) 11906.
- [24] G. Pacheco, E. Zhao, E. Diaz Valdes, A. Garcia, J.J. Fripiat, *Microporous Mesoporous Mater.* 32 (1999) 175.
- [25] J.L. Kurz, *J. Phys. Chem.* 66 (1962) 2239.
- [26] F. Feigl, *Spot Tests in Inorganic Chemistry*, 5th ed., Elsevier, Amsterdam, 1958.
- [27] M. Yada, H. Kitamura, M. Machida, T. Kijima, *Langmuir* 13 (1997) 5252.
- [28] P.C.A. Alberius, K.L. Frindell, R.C. Hayward, E.J. Kramer, G.D. Stucky, B.F. Chmelka, *Chem. Mater.* 14 (2002) 3284.
- [29] M.H. Huang, B.S. Dunn, H. Soye, J.I. Zink, *Langmuir* 14 (1998) 7331.
- [30] B.E. Warren, *Phys. Rev.* 59 (1941) 693.

- [31] L.A. Smith, R.B. Hammond, K.J. Roberts, D. Machin, G. McLeod, *J. Mol. Struct.* 554 (2000) 173.
- [32] Neeraj, C.N.R. Rao, *J. Mater. Chem.* 8 (1998) 1631.
- [33] M. Tiemann, M. Fröba, G. Rapp, S.S. Funari, *Chem. Mater.* 12 (2000) 1342.
- [34] C.J. Brinker, G.W. Scherer, *Sol-Gel Science*, Academic Press, Boston, 1990, p 251.
- [35] P.E. Quintard, P. Barbéris, A.P. Mirgorodsky, T. Merle-Méjean, *J. Am. Ceram. Soc.* 85 (2002) 1745.
- [36] G.Y. Guo, Y.L. Chen, W.J. Ying, *Mater. Chem. Phys.* 84 (2004) 308.